Electronic transport in a model tetraphenylbenzidine main-chain polymer: Direct comparison of time-of-flight hole drift mobility and electrochemical determinations of hole diffusion

M. A. Abkowitz, J. S. Facci, W. W. Limburg, and J. F. Yanus
Xerox Webster Research Center, 114-39D, 800 Phillips Road, Webster, New York 14580
(Received 5 December 1991; revised manuscript received 19 May 1992)

Electronic transport behavior is analyzed in a model polytetraphenylbenzidine (PTPB) hole transport polymer in which electroactive tetraphenylbenzidine sites are covalently bonded within the polymer main chain. Time-of-flight (TOF) techniques are used to measure the hole drift mobility as a function of electric field and temperature. The TOF data are parametrized using the phenomenological model originally proposed by Gill. For comparative purposes, the disorder model developed by the Marburg group is also used to analyze the data. Transport of holes in PTPB is demonstrated to occur via hopping among the TPB functional units. A pattern of convoluted field and temperature-dependent features, now known to be shared by a broad class of disordered molecular materials, is revealed by the TOF data. Thin solid film electrochemical techniques are applied in parallel with the TOF technique to independently obtain hole diffusion coefficients (D_h) in thin films of PTPB. As a unique consequence of this comparison, it is established that mobilities, computed from solid-state hole diffusion data using the Einstein relation, converge with zero-field extrapolated TOF mobilities over a wide temperature range when the extrapolation is computed from $\log \mu$ vs $E^{1/2}$ plots. Therefore, the functional dependence of the logarithm of the drift mobility on the square root of field, a much discussed general feature of electronic transport in disordered molecular materials, is demonstrated to persist through the critical low-field limit. At the same time it is demonstrated that the contribution of thermally driven diffusive broadening, which can now be calculated directly from the independently determined electrochemical hole diffusion coefficients, makes an insignificant contribution to the experimentally observed width of the time-of-flight transit pulse. A comparison of the PTPB data with analogous TOF data on solid solutions of TPD (the functional unit in PTPB) dispersed in polycarbonate is described. The observation that hole drift mobilities in PTPB are an order of magnitude smaller than those in the corresponding TPD-polycarbonate solid solution is discussed in terms of disorder and steric constraints.

I. INTRODUCTION

We have been engaged in exploiting and developing a complementary combination of electrochemical and solid-state physics techniques as a unique means of probing the mechanistics of electronic hopping transport in glassy polymeric materials.[1-4] Glassy transparent solution coatable polymers capable of transporting an injected charge with negligible loss to deep traps are of critical importance in electrophotography and certain of these have been extensively[5-23] studied by time-of-flight (TOF) drift-mobility and xerographic techniques. Such measurements made in the course of technically evaluating a wide variety of amorphous organic systems, including molecularly doped polymers, pendant polymers, and main-chain polymers, clearly reveal a recurrent pattern of features[6,22] in the field and temperature dependence of mobility. The extent to which these features depend solely on disorder or whether they depend additionally on the steric and molecular relaxational properties of the system has become a subject of fundamental interest.[23]

In transport studies on a wide variety of disordered molecular materials the observation which has excited the greatest interest and has posed a singular problem for theory is the ubiquitously observed square-root field dependence of the logarithm of the TOF drift mobility.[6,22,23] A clear understanding of the origin and functional form of the field dependence does not yet exist despite several theoretical attempts[24,25] to explain its origin. Also unresolved is a key and related experimental question, namely the extent to which this functional behavior continues to apply throughout the low-field limit. As a practical matter, it has generally proven difficult to extend TOF measurements significantly below 10^3 V/cm. It is precisely in this low-field regime where TOF drift-mobility measurements are rendered ambiguous by space-charge and finite conductivity effects, phenomena which are particularly exacerbated at low temperature. This inability to extend TOF drift-mobility measurements to low field is the primary motivation for the present attempt to utilize electrochemically measured electronic diffusion coefficients as a means of evaluating the mobility in zero-field limit. Shown below in diagram 1 is the molecular structure of the electrochemically reactive polytetraphenylbenzidine (PTPB) hole-transport polymer which provides the venue for the comparison of hole mobilities with hole diffusion coefficients D_h.

Electronic diffusion coefficients in electroactive polymers are electrochemically characterized by an electron (D_e) or hole (D_h) diffusion coefficient depending on whether the hopping sites can be electrochemically reduced (electron added) or oxidized (electron removed), re-

spectively. The diffusion of holes in the present study is driven exclusively by a concentration gradient of oxidized and unoxidized (neutral) hopping transport sites. Hole diffusion coefficients can now be experimentally measured by an array of electroanalytical techniques including potential step chronoamperometry[26] and a family of steady-state voltammetric techniques which are based on the use of two terminal interdigitated arrays (IDA's) or twin electrode sandwich cells[27–32]. All electrochemical measurements of hole diffusion coefficients involve bulk electrolysis of the transport sites, so it is important to note that counterions, which are Coulombically bound to the electrically charged oxidized transport sites, are not only unavoidably imbibed into the film during the electrochemical experiments but are also required to conduct the diffusion measurements. Steady-state electroanalytical techniques[27–29] are employed in this paper because these techniques avoid any complication which may result from the coupling of electronic hopping to the mass transport of counterions. These electroanalytical techniques are now being widely applied to the measurement of charge-transport rates in electroactive[27–32] and conducting polymers.[33–36]

In PTPB it is demonstrated that the square-root field dependence of the logarithm of mobility is sustained to the zero-field limit. This result simultaneously embodies an experimentally direct and self-consistent verification of the Einstein relation between diffusivity and mobility in an organic glass. It follows directly from the electrochemical data that a mechanism of simple thermal diffusive broadening fails by some orders of magnitude to account for the experimentally observed TOF transit pulse shapes in PTPB. This observation supports the presumption, based on a number of recent studies,[5,8] that the indicated broadening is a general characteristic of molecular materials, which otherwise exhibit a well-defined transit time obeying the conventional scaling laws. Also provided below are comparative studies of PTPB with solid solutions of the analogous TPD (the functional unit in PTPB) species (diagram 1) dispersed in a polycarbonate matrix:

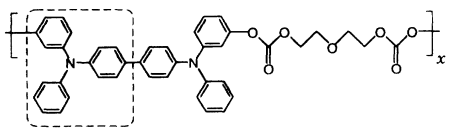

PTPB

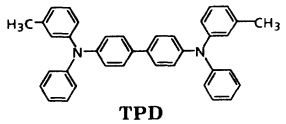

TPD

The comparison demonstrates that the electroactive TPB sites, which are covalently bonded within the main chain of the polymer, serve as the molecular sites for electronic transport. (The part of the molecule within the dashed figure is a triarylamine group which can be oxidized to the radical cation and represents the basic hole hopping site.) This comparison affords an additional opportunity to compare electronic transport among sterically constrained hopping sites in PTPB with hopping in an analogous but less constrained system.

II. EXPERIMENT

A. Materials and film preparation

The PTPB polymer was synthesized by the condensation of *N,N'*-diphenyl-*N,N'*-di-m-hydroxyphenyl-4,4'-diaminobiphenyl, *m*-(OH_2)TPB, with diethyleneglycolbis(chloroformate), $[ClC(O)CH_2CH_2]_2O$. The details of the synthesis are described elsewhere.[37] Smoth uniformly thick films of PTPB are formed by casting a solution of the polymer in chlorobenzene onto the substrate and allowing the solvent to slowly evaporate. For time-of-flight experiments, PTPB films on the order of 15 μm are draw-bar coated from a chlorobenzene solution onto 100-nm-thick Au films which were electron-beam deposited onto highly polished single-crystal Si wafers. A Cr adhesion layer was first applied to the wafer as an aid in bonding the Au film. An Al top contact is thermally evaporated onto the dry polymer film. For electrochemical experiments, thin (ca. 200 nm) films of PTPB were solvent cast onto the interdigitated arrays by evaporation from a dilute (1–5 mg/ml) chlorobenzene solution of the polymer. Evaporation was purposely slowed by saturating the local atmosphere with chlorobenzene vapor. An anhydrous $LiClO_4$ electrolyte, used in electrochemical experiments, was used as received but dried *in vacuo* at 110 °C immediately prior to use. High purity acetonitrile, specified to contain less than 0.015% water, was used as received. All other materials were generally of the highest purity available.

B. Mobility measurements

Drift mobilities were measured by the canonical small signal current mode time-of-flight (TOF) technique. Figure 1 illustrates the experimental arrangement for TOF measurements. Sample films were fitted with an electrically blocking, semitransparent aluminum contact configured into a sandwich geometry. The capacitorlike specimen (capacitance C_s) in series with a switched power supply and sensing resistor R was then excited by a weak pulse of strongly absorbed 337-nm light from a ni-

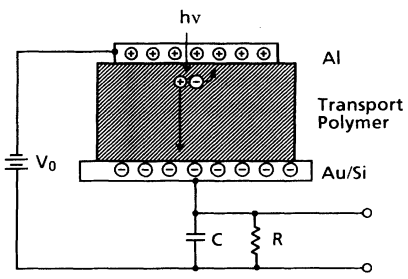

FIG. 1. Schematic diagram of the experimental arrangement for TOF measurements made on PTPB polymer films. The value C is the lumped capacitance of the input circuitry including the transient digitizer.

trogen laser at some experimentally controlled time after the application of a dc bias V_0. The parameter C in the figure represents the additional circuit capacitance. The drift of a unipolar sheet of carriers from the photoexcited contact region through the film bulk in uniform field induces a transient voltage to appear across the sensing resistor which is amplified, digitized, and processed. The value of the sensing resistor was adjusted to keep the overall circuit time constant much less than an experimental transit time (i.e., current mode TOF). The intensity of the incident light flash was such that the integrated quantity of the photogenerated charge in transit was less than 0.1 $C_s V_0$ ($C_s V_0$ is the charge residing on the specimen electrodes after application of bias V_0) to ensure uniformity of the internal field (i.e., small signal conditions). The specimen temperature was held to within 0.5 K in a variable temperature chamber continuously flushed with dry nitrogen. The transit time could be determined directly from the transit pulse shapes which were examined as a function of field and temperature. The integrated exposure of any sample film to uv radiation was kept low enough to preclude photodegradation.

C. Electrochemical measurements of diffusion

Electrochemical determination of hole diffusion coefficients are obtained from smooth uniform thin films (ca. 200 nm) of solvent-cast PTPB which are coated onto a microelectrode interdigitated array (IDA), shown schematically in Fig. 2. Details of the IDA fabrication process are presented elsewhere.[3] The microlithographically patterned IDA is composed of 50 inner and 51 outer gold microelectrodes, which form the two terminals (W_1 and W_2) of the array. Each of the microelectrodes is 5 μm wide, 1000 μm long, and 100 nm thick. The edge-to-edge interelectrode separation is 5 μm. The IDA's are fabricated on a 500-nm-thick thermal SiO_2 layer on a $\langle 100 \rangle$ single-crystal 3-in. silicon substrate. Adjacent microelectrodes are electrically insulated from one another by the thermal oxide. The device lead-in lines were carefully overcoated with a silicone adhesive under a 30× stereomicroscope in order to mitigate unrelated electrochemical responses from these electrodes.

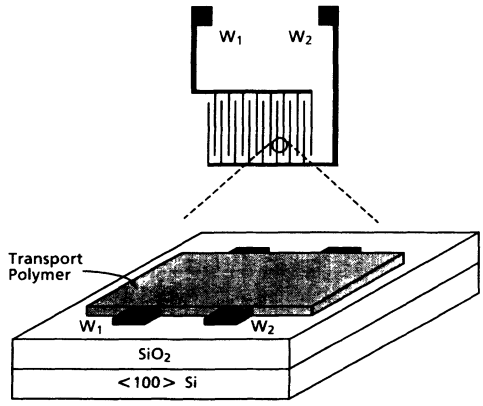

FIG. 2. Schematic diagram of the experimental arrangement for electrochemical measurements of the hole diffusion coefficient in PTPB polymer films. Thin films of PTPB are coated onto a microelectrode interdigitated array.

The PTPB polymer film is cast over both the microelectrodes and the insulating SiO_2 area between microelectrodes. Due to their proximity, adjacent microelectrodes become physically bridged by and electrically connected with PTPB. Independent electrolysis potentials are applied to the arrays such that the terminals W_1 and W_2 function as hole generator and collector electrodes, respectively. The overcoated array is immersed in an inert electrolyte, 0.3 M lithium perchlorate in acetonitrile solvent. Holes which are generated at a given microelectrode, diffuse toward and are collected at an immediately adjacent microelectrode. All electrolysis potentials are referenced against a saturated calomel electrode (SCE). Variable temperature measurements were made using a nonisothermal electrochemical cell arrangement in which the reference electrode was kept at room temperature while the cell temperature was varied.

In addition to these in-electrolyte measurements, hole diffusion coefficients were measured in the solid state as follows. Briefly, a thin film of PTPB, overcoated onto an array, was half-oxidized and removed under potential control from the acetonitrile electrolyte, rinsed, dried, and introduced into a cell containing only acetronitrile vapor. Current-voltage curves are obtained on the array in the usual two-electrode configuration. The details are presented below.

III. RESULTS AND DISCUSSION

A. Mobility measurements

Figure 3 illustrates a typical TOF transient line shape obtained on PTPB. Transit time data were obtained directly from clearly discernible features of the real-time transients, rather than from a log$i$ vs log$t$ representation of the data. It is emphasized that analyses carried out on

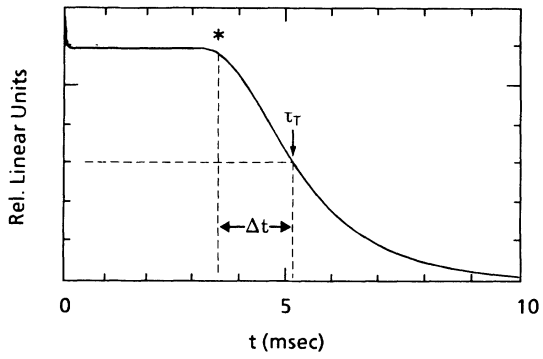

FIG. 3. Time-of-flight transit pulse shape. The ordinate is in relative linear units. The time of arrival of the fastest carriers highlighted by the asterisk is about 3.5 msec. The mean transit time τ_T (5 msec) is taken to be the time at which the current drops to half of the value at the plateau. The relative dispersion $\Delta t/\tau_T$ (~ 0.3) is defined as the ratio of the carrier dispersion Δt (difference between the time of arrival of the fastest carriers and τ_T) to the mean transit time.

a series of specimens varying in thickness revealed none of the anomalous scaling behavior characteristic of dispersive transport that would require a log-log representation to determine a transit time.[38] The latter is not surprising because the plateau on the transient is characteristic of a transport process in which the injected carriers come into equilibrium with the transport controlling electronic states in a small fraction of a transit time. In other words, a quasiequilibrium is established before the carriers have penetrated much beyond the generation zone adjacent to the illuminated surface.

The knee of the curve in Fig. 3 gives the arrival time ($\sim$3.5 msec) of the fastest carriers. The mean arrival time defined as the transit time τ_T of the carrier packet is the time at which the current has dropped to half its initial value and is about 5 msec for the specimen in the figure. The difference between the fastest arrival time and the transit time Δt is a measure of the dispersion of the carrier packet. The relative dispersion of the transiting carriers $\Delta t/\tau_T$ is therefore is 0.3. Transit time and relative dispersion data were collected as a function of electric field, temperature, and specimen thickness.

B. Field and temperature dependence of mobility

Experimental data are typically represented as a family of logarithmic mobility versus logarithmic field plots parametric in temperature. This data can be systematically deconvoluted to reveal much more clearly the underlying pattern of behavior. As is the case with many other disordered molecular materials,[6] the combined field and temperature dependence of the hole drift mobility can be described by the phenomenological equations [Eqs. (1a) and (1b)]

$$\mu=\mu_0\exp[-(\varepsilon_0-\beta E^{1/2})/k_B T_{\text{eff}}]\ , \tag{1a}$$

$$1/T_{\text{eff}}=1/T-1/T_0\ , \tag{1b}$$

originally proposed by Gill[39] to describe the drift-mobility data in polyvinylcarbazole (PVK). Thus, Fig. 4 presents a plot of the logarithm of drift mobility versus the square root of field parametric in temperature. The slopes of the plots in Fig. 4 clearly increase with diminishing temperature. This behavior is explicitly illustrated in the inset which presents these slopes against reciprocal temperature. Note that the latter plot extrapolates to zero at about 410 K. Zero-field hole drift mobilities ($\mu_{E=0}$) were estimated by extrapolating to zero field the square-root ($E^{1/2}$) representation of the data. These are represented by the highlighted symbols on the $E=0$ axis.

The functional form of the temperature dependence of the hole drift mobility is presented in Fig. 5. The figure, which shows a family of plots of the logarithm of mobility versus reciprocal temperature parametric in applied field, clearly reveals that the temperature dependence of drift mobility can be represented as Arrhenius activated, that the effective activation of the hole drift mobility decreases as the field increases, and that the various plots extrapolate to a common intersection at about 410 K. In the inset to Fig. 5, field-dependent activation energies (unfilled points), obtained from the slopes of the plots in the figure, are plotted against the square root of the applied field. The solid line is a linear least-squares fit to the field-dependent activation energies. The value of the zero-field activation $\varepsilon_0=0.53$ eV is shown by the symbol on the zero-field axis and is determined from an Ar-

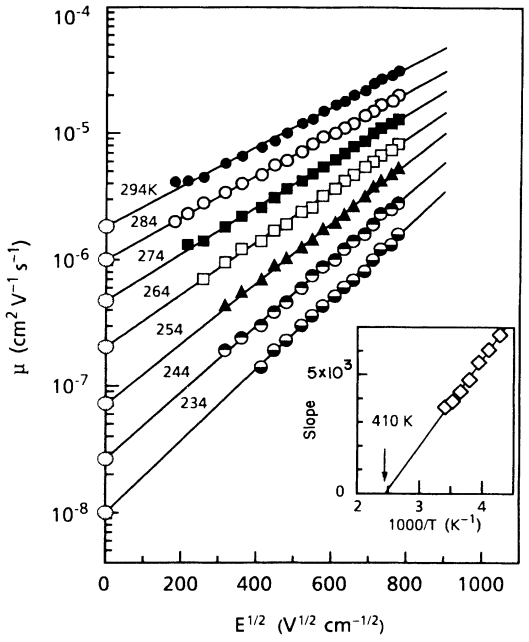

FIG. 4. Logarithm of the TOF drift mobility vs the square root of the applied field at various temperatures. The inset shows the slopes of the logarithmic mobility vs square-root field plots plotted against inverse temperature. A linear fit extrapolates to zero at 410 K.

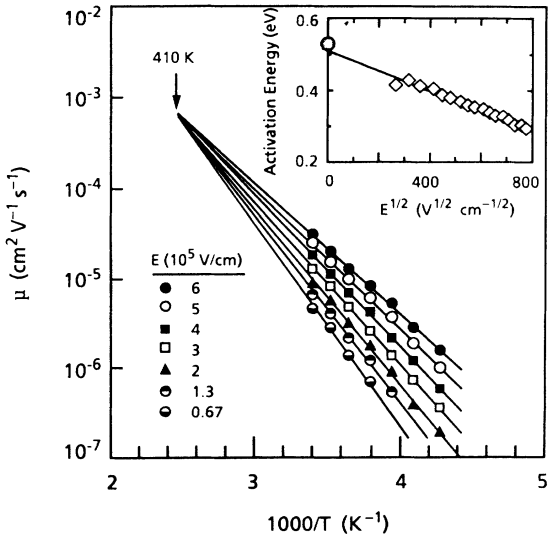

FIG. 5. Arrhenius plots of the TOF hole drift mobility in PTPB. The plots are parametric in the applied field. Inset: activation energies, computed from the slopes of the Arrhenius plots plotted against the square root of the field. The symbol on the zero-field axis is the activation energy determined from an Arrhenius plot of the zero-field data in Fig. 4.

rhenius plot of the extrapolated zero-field mobility values highlighted in Fig. 4. For comparative purposes the corresponding zero-field activation, based on a linear rather than a square-root extrapolation, is 0.45 eV.

The remaining parameters μ_0, β, and T_{eff} from Eq. (1) are determined from Figs. 4 and 5. The parameter β is obtained from the slope of the activation versus field data (or alternatively from an analysis of Fig. 4) and is 0.32 meV/(V/cm)$^{1/2}$. The temperature shift factor T_0, which is obtained from the intercept on the reciprocal temperature axis in Fig. 4, is 410 K. By comparison, the glass transition temperature of PTPB, obtained from differential scanning calorimetry, is 380–386 K. Finally, the mobility prefactor $\mu_0 \sim 10^{-3}$ cm^2 V^{-1} s^{-1} is also determined from the extrapolated intersection of the data at $T = T_0$ in Fig. 5.

The form taken by the field-dependent effective activation in Eq. (1) suggests comparison with the Poole-Frenkel[37] parameter β(PF), Eq. (2),

$$\beta(\text{PF}) = (e^3/\pi\varepsilon_0\varepsilon)^{1/2} . \quad (2)$$

For the relative dielectric constant $\varepsilon = 3.0$, one obtains $\beta(\text{PF}) = 0.45$ meV/(V/cm)$^{1/2}$, which is only somewhat larger than the measured value of $\beta = 0.32$ meV/(V/cm)$^{1/2}$. As noted in similar analyses carried out on other glassy molecular materials,[5] outstanding questions remain regarding the applicability of the Poole-Frenkel[40] model to disordered transport polymers. The Poole-Frenkel model and its several variants, in fact, require the questionable existence of Coulombic centers (traps which are charged when empty) which must be perfectly compensated under equilibrium conditions and the improbable feature that their concentration must somehow remain invariant among specimen films.

Although quite intricate, the pattern of electronic charge-transport behavior embodied in the Gill equation and illustrated above for PTPB in Figs. 4 and 5 exhibit the following key transport characteristics: (1) the hole drift mobility is thermally activated; (2) the activation energy is field dependent; (3) the hole mobility is field dependent, best conforming to a $\log\mu$ vs $E^{1/2}$ relationship throughout the experimentally accessible range of fields; (4) the slopes of these plots scale as $1/T$. It should be emphasized that while the Gill equation is useful in organizing experimental data for comparative purposes, the microscopic origin of the underlying behavior it describes remains uncertain. The many other materials which share in precise detail the features embodied in Eq. (1) differ very widely in chemical composition and morphology. These include (i) pendant polymers like PVK (Ref. 39) where the transport-active moiety is pendant from an inert main chain, (ii) solid solutions of a transport-active molecule dispersed in an inert glassy polymeric matrix, e.g., TPD in polycarbonate,[41] (iii) Si and Ge backbone polymers[5,6] in which it has been established that transport occurs via polymer-backbone-derived states and in which the side groups play a subsidiary role.

The experimentally observed thermally activated drift mobility is readily recognized as the signature of a transport process mediated by interaction with localized states. This could implicate three distinct transport processes. These are (1) trap-controlled band transport, in which the activation energy is a measure of the mean displacement of the trap manifold from the band edge, (2) small polaron hopping, and (3) hopping in a manifold of localized states which might not exhibit site relaxation but are always made energetically inequivalent by disorder. Trap-controlled band transport is thought to be least likely for two reasons. First, the polymer PTPB is amorphous (no evidence can be found from differential scanning calorimetry for any crystallinity). Even a perfectly ordered (crystalline) analog of PTPB would have a very narrow bandwidth (0.05–0.10 eV). Thus under these circumstances, the superposition of even a modest disorder potential would act to localize all the states in the band. It is therefore not anticipated that band transport can survive as a microscopic mechanism in amorphous PTPB. Second, the quantitative characteristics of transport in PTPB remain invariant among a wide range of specimen films prepared at different times from different source batches. A trap-controlled process would be expected to show random quantitative variations in the transport parameters as the number of such trapping sites would certainly vary among specimen films. The transport process then most likely remains hopping. The functional unit in PTPB is the aromatic diamine tetraphenylbenzidine. The molecularly doped polymer consisting of TPD (see diagram 1) dispersed in a polycarbonate matrix exhibits transport characteristics identical to those of PTPB. In the molecularly doped polymer it has been incontrovertibly established that transport proceeds by a thermally assisted hopping process.

In a polaronic picture, it is presumed that a charge carrier localized on the triarylamine functional unit in PTPB interacts strongly with both the molecular vibronic excitations of the site and quite possibly those of the surrounding medium (outer-shell processes). These interactions self-trap the charge carrier which can now move only as a quasiparticle dragging along its local distortions. A particular model of the small polaron model developed by Holstein[42] and later by Emin[43] has been applied with some success to transport in certain molecularly doped polymer by Schein and co-workers.[18–20] Key to their assignment of a polaronic process, however, is their ability to isolate and identify changes in the transport parameters (i.e., hopping probability and effective activation) induced by systematically varying intersite separation. The latter is accomplished by simply changing the small molecule doping level in a glassy binder. In the present study, a similar analysis is precluded. Here we are obliged to deal with the fact that site separation of functional units on the PTPB chain is clearly a fixed feature of the composition. Thus the relative importance of site relaxation and disorder to the hopping transport process cannot be definitively established by mobility measurements alone. It should be emphasized that simple polaron theory predicts a field dependence of the form $E^{-1}\sinh(aE)$ inconsistent with the present measurements of drift mobility and certainly with the zero-field mobilities estimated in Fig. 5.

The general applicability of the Gill equation suggests a common microscopic mechanism underlying the trans-

port process in diverse molecular media. These solids clearly share the following two characteristics: (1) transport proceeds by a thermally activated hopping process and (2) disorder. Both features are incorporated in a disorder model developed by the Marburg group[11] which is based on Monte Carlo simulations of hopping transport. The appeal of this model derives from its attempt to describe the field and temperature dependence of the drift mobility as well as the details of the transit pulse shape, including the temperature at which a transition to dispersive transport should take place, solely in terms of the disorder inherent in the system.

In this model[11] holes are injected at some arbitrary energy into an empty manifold of localized states, characterized by a Gaussian distribution of energies. The width of the Gaussian manifold σ is essentially a measure of the energetic disorder of the hopping sites. The injected carrier then thermalizes within this manifold of states and relaxes to a dynamic equilibrium at a level $\langle \varepsilon_\infty \rangle$,

$$\langle \varepsilon_\infty \rangle = \sigma^2 / k_B T \ , \tag{3}$$

which is measured relative to the center of the Gaussian density of states. Note that carrier interactions (correlated hopping effects) are excluded from consideration. Because the mean energy attained by the transiting carrier depends on temperature, the temperature dependence of drift mobility ceases to be simply activated. The model instead predicts that

$$\mu = \mu_0 \exp[-(T_0^{\text{eff}}(E)/T)^2] \ , \tag{4}$$

where $T_0^{\text{eff}}(E)$, given by the expression in Eq. (5),

$$T_0^{\text{eff}}(E) = T_0(1 - BeaE/\sigma) \ , \tag{5}$$

is a measure of the width of the distribution expressed as a temperature. The prefactor μ_0, the mobility when $1/T^2 \to 0$, corresponds to the perfectly ordered analog system. In the disorder model, the electric field acts to lower the barriers to hopping up in energy in the field direction thereby effectively reducing the width of the Gaussian distribution. In the framework of this model the field and temperature dependence of the mobility is expressed as

$$\mu = \mu_0 \exp[-(T_0/T)^2] \exp(E/E_0) \ , \tag{6}$$

where

$$E_0 = \sigma / 2Bea (T/T_0)^2 \ . \tag{7}$$

Here a is the intersite distance and B is a numerical correction factor that accounts for the fact that only jumps in the field direction are assisted.

The reanalysis of experimental PTPB data within the framework of the disorder model leads to an estimate of the energetic disorder parameter σ characteristic of this polymer. Figure 6 replots the PTPB data of Fig. 5 as a function of $1/T^2$ subject to the constraint that the data extrapolate to a common intercept at $1/T^2 = 0$. Over the experimentally accessible temperature range it clearly is not possible to assign greater credibility to either a conventional Arrhenius temperature dependence or the form indicated in Eq. (4).

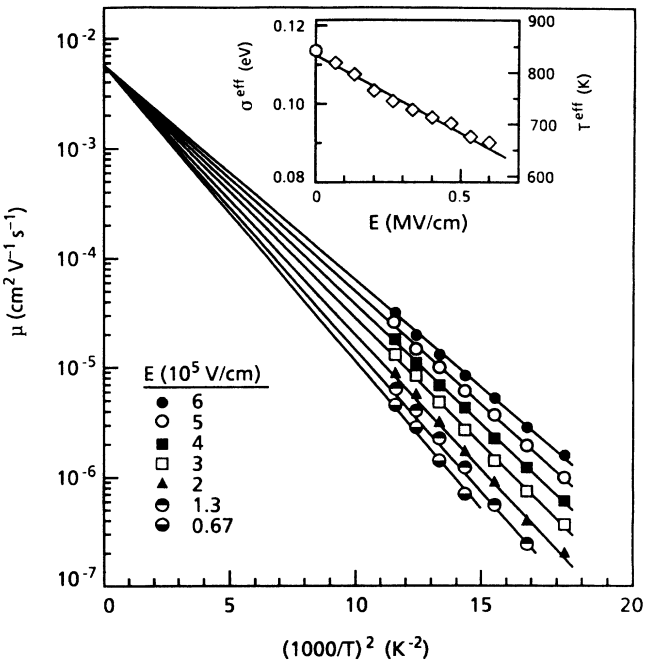

FIG. 6. Logarithm of the hole drift mobility in PTPB vs $1/T^2$ parametric in the field. The linear fits are subject to the constraint of a common intercept at $1/T^2 = 0$. The inset shows σ^{eff} (left-hand-side axis) and equivalent values of T^{eff} (right-hand-side axis) plotted against the field.

The data in Fig. 4 were replotted as $\log\mu$ against E (instead of $E^{1/2}$) and the logarithm of the zero-field mobility was then estimated from this linear field extrapolation. The zero-field mobility plotted against $1/T^2$ then yields from Eq. (6) the effective width of the distribution of hopping sites, expressed as an effective temperature T_0. Thus it was determined that $T_0 = 898$ K at $E = 0$. This value of T_0 is equivalent to a $\sigma = 0.11$ eV at zero field. At finite fields, the parameters $T_0^{\text{eff}}(E)$ are determined from the slopes of Fig. 6 according to Eq. (4). The inset to Fig. 6 is then a representation of the field dependence of the effective width of the distribution of hopping sites against field. The mobility prefactor $\mu_0 = 7 \times 10^{-3}$ cm^2/V sec. We note for comparison that similar analyses yields $\sigma = 0.15$ eV for PVK and $\sigma = 0.09$ eV for polymethylphenylsilane[5] (PMPS). Of the three systems just described, the predicted energetic disorder is evidently greatest in PVK and least in PMPS. It is interesting to note that these observations are consistent with the fact that the broadening of the TOF transit pulse is, correspondingly, greatest in PVK and least in PMPS under essentially identical experimental conditions.

In the original formulation of the disorder model as expressed in Eqs. (3)–(7), the appropriate extrapolation of drift mobilities to zero field would be linear not square root, as clearly suggested by the experimental data. In a more recent embodiment of the model, however, Pautmeier, Richert, and Bässler[24] have included the influence

of random fluctuations of the wave-function overlap parameter (off-diagonal disorder) in addition to energetic (diagonal) disorder. Depending, in this case, on the relative values of energetic and spatial disorder, the logarithmic mobility is predicted to exhibit a more complex sigmoidal field dependence with the attendant possibility of saturation at low field.

Neither simple polaron models, nor the disorder model, nor the multitude of models based on electron self-exchange, nor even very recent models which treat the hopping sites as dipolar centers, are able account for the type of field dependence observed in TOF if in fact this behavior persists to zero field. The present comparison between TOF drift mobility and electrochemical diffusion data in a redox, hole transporting polymer serves to provide the first direct experimental evidence that this can indeed be the case.

C. Electrochemical measures of diffusion coefficients

Two electrochemical techniques for the measurement of hole diffusion coefficients in PTPB are now presented and compared. Briefly, in the classical in-electrolyte technique, hole diffusion coefficients are obtained with a PTPB-coated IDA immersed in an inert electrolytic solvent (0.3 M $LiClO_4$ in acetonitrile). In the more recently developed solid-state technique,[27–29] the liquid electrolyte is absent and, as a consequence, the PTPB specimens are relatively less plasticized. These unplasticized specimens much more closely resemble the thin solid films used for the TOF measurements. Although details of the measurement technique are presented elsewhere,[2,3,27] it suffices to say here that both electrochemical techniques provide a means of sustaining a steady-state concentration gradient of charged hole transport sites (oxidized radical cation derivatives of the neutral functional sites).

1. In-electrolyte diffusion coefficients

This set of experiments is based on the fact that the charge (or oxidation) state of an electroactive film mounted on an electrode and immersed in an electrochemical cell can be precisely controlled by means of an electrode potential applied with respect to a reference electrode in the same solution. Electroactive films on electrodes are redox active only over a narrow range of electrochemical potentials (ca. 300 mV). The ratio of oxidized (radical cation) to reduced (neutral) species at the electrode-polymer interface is exclusively governed by the applied potential (as ideally expressed by the Nernst equation[26]). This ratio is, in effect, instantaneously responsive to changes in the electrode potential.

In measurements involving the polymer-coated IDA, two potentials are now independently applied to the two array terminals (see Fig. 2). The concentration of oxidized (or reduced) hole-transport sites at the W_1-polymer and W_2-polymer interfaces are thus controlled by application of independent electrode potentials V_1 and V_2, respectively. The concentration of oxidized hole-transport species at these interfaces can be purposely made different by respectively applying different electrode potentials V_1 and V_2 relative to a common reference electrode. Under these conditions a concentration gradient of hole transport species is generated in the bulk of the film between the two electrodes W_1 and W_2. In the present experiments the potential V_2 is fixed at a reducing potential of 0.3 V vs SCE while the electrode potential V_1 is varied very slowly during which time the hole current from W_1 to W_2 is simultaneously measured. The resulting current-potential plot is shown in Fig. 7. It was demonstrated experimentally that when V_1 is swept under the latter quasistatic conditions, the current displayed at any given voltage (Fig. 7) is identical to the current measured under true steady-state conditions (sweep turned off). Under the circumstances just described and for any pair of voltages V_1 and V_2 a linear concentration gradient of oxidized (or reduced) hole-transport sites is maintained. A maximum in the steady-state concentration gradient is achieved when all the hole-transport sites at W_1 are oxidized corresponding to $V_1 = 1.1$ V and correspondingly all the hole-transport sites at W_2 are reduced ($V_2 = 0.3$ V). When V_1 is increased beyond 1.1 V, a further increase in the concentration gradient cannot be effected. The electronic diffusion current illustrated in Fig. 7 is therefore maximized at 1.1 V since further increase in V_1 cannot influence the concentration gradient.

Note that in these measurements the IDA is present in an electrolytic solution containing a high concentration of cations and anions which are rapidly imbibed into and are highly mobile within the thin polymer film, as required to maintain microscopic and overall charge neutrality. As a result at any given pair of voltages V_1 and V_2, the fixed-site radical cations are exactly Coulombically compensated by the counterions whose stationary spatial distribution is coupled and therefore parallel to the concentration gradient of radical cations. The availability and mobility of electrolyte ions ensures electric field collapse in the bulk of the film. Under these conditions the steady-state current measured between W_1 and W_2 is an electronic *diffusion* current, and in the present case a hole diffusion current.

At any given temperature T, therefore, the in-

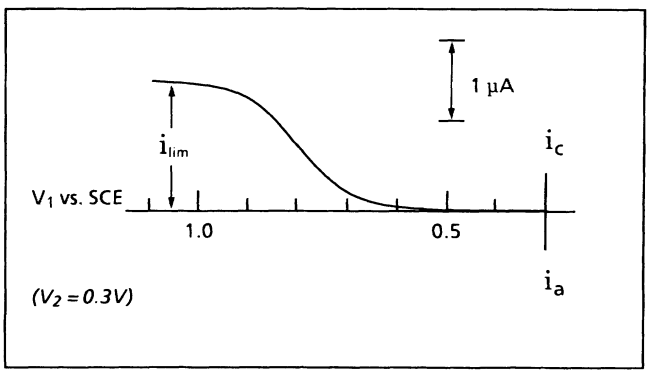

FIG. 7. Steady-state current-voltage plot for a PTPB-coated IDA immersed in an inert electrolytic solvent. The figure plots the anodic current at W_1 vs the electrode potential V_1 applied to W_1; V_2 is fixed at 0.3 V vs SCE.

electrolyte hole diffusion coefficients $D_h(T)$ in PTPB is computed from the limiting-current value i_{lim} obtained from the quasi-steady-state current-voltage curve presented in Fig. 7. This limiting current i_{lim} is related to D_h by Fick's first law[26] which is recast as Eq. (8),

$$i_{lim} = nFAC_{tot}D_h/d \ . \tag{8}$$

In Eq. (8) d is the edge-to-edge spacing of the microelectrodes (5 μm), $n=1$, $C_{tot}=3.2\times10^{-3}$ mole/cm^3 expressed as a triarylamine site concentration, and A is the effective electrode area of the microelectrodes given by the sum of the areas of the 0.1-μm-high electrode facets. The total electrode area is given by $A=hl(N-1)=10^{-4}$ cm^2 where h is the thickness of the Au microelectrodes (10^{-5} cm), l is the length (0.1 cm), and N is the number of microelectrodes ($N=101$). From the experimentally determined limiting current, $i_{lim}=1.6$ μA, a value of $D_h=3.3\times10^{-8}$ cm^2/s is obtained. Hole diffusion in PTPB is observed to be thermally activated. Under these circumstances the temperature-dependent diffusion coefficients can be represented by the equation $D_h=D_h^0\exp(-\Delta H^*/kT)$, where D_h^0 is the infinite-temperature hole diffusion coefficient and ΔH^* is the hopping activation enthalpy. The slope of an Arrhenius plot of the diffusion coefficients, shown in Fig. 8 curve B (solid circles), reveals that $\Delta H^*=0.31$ eV.

2. *Solid-state diffusion coefficients*

The electrochemical technique for the measurement of hole diffusion coefficients in the solid state is similar to that described above but with two important differences: (1) the liquid electrolyte is absent during the measurement of diffusion current and (2) the film is on an "ion budget".[44] The latter means that the number of counterions is experimentally fixed and equal to the number of triarylamine radical cations. Hence the total number of oxidized triarylamine functional groups within the film (half-oxidized in the present case) does not vary with the applied potential difference V_2-V_1.

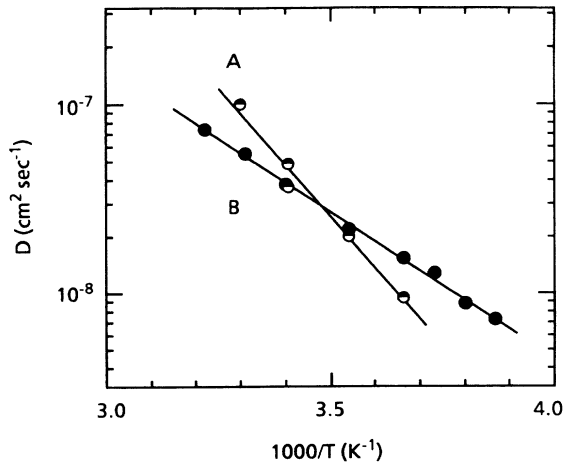

FIG. 8. Arrhenius plot of the electrochemically measured hole diffusion coefficients in PTPB: A, in the dry solid state but exposed to an acetonitrile vapor in argon and B, when immersed in an inert electrolytic solvent.

The sample preparation for the measurements begins by oxidizing exactly one-half of the triarylamine groups in a PTPB film coated onto a IDA immersed in an electrochemical cell (i.e., in contact with a liquid electrolyte) by applying a potential of 0.83 V vs SCE to both (or either) of W_1 and W_2. It should be realized that the ratio of oxidized to reduced species ultimately relaxes to a constant value everywhere within the film, the value being given by the magnitude of the applied electrode potential. That is, the concentration of oxidized or reduced transport sites ultimately becomes constant throughout the bulk of the PTPB film. The film-coated IDA is then emersed from the cell under potential control. After the film is completely removed from the electrolyte the IDA is in effect electrically disconnected. Hence further changes in the concentration of the radical cation are precluded. The excess $LiClO_4$ electrolyte, which remains in the film after the volatile acetonitrile solvent has evaporated, is then removed by repeated immersion in pure electrolyte-free acetonitrile. The concentration of radical cations in the film is not influenced by this step. The concentration of counterions at this point exactly counterbalances the number of charged transport sites.

The half-oxidized PTPB-coated IDA is then reintroduced into the original electrochemical cell which contains only an atmosphere of argon saturated with acetonitrile vapor. The net effect of contacting the specimen with acetonitrile vapor is to render mobile the charge compensating perchlorate anions which are resident in the PTPB film. An interelectrode potential $\Delta V=V_1-V_2$ is then applied across W_1 and W_2 and is swept slowly (quasistatically). As a consequence of the mobility of the counterions, the applied potential ΔV is dropped across each electrode-polymer interface. Thus the application of a nonzero ΔV across the half-oxidized film leads to an electrolytic electrode reaction at each electrode-polymer interface: oxidation of neutral triarylamine groups to the radical cation occurs at the anode (positive electrode) and a corresponding reduction of oxidized radical cations to the neutral triarylamine species occurs at the cathode (negative electrode). The facile mass transport of counterions in the half-oxidized film additionally ensures that the oxidized transport sites remain charge compensated at all times during the quasistatic potential sweep and that the concentration gradient of radical cations will readjust to continuous changes in the interelectrode potential. Under these circumstances, therefore, the concentration gradient of oxidized transport sites and counterions are parallel and the applied potential is dropped at the interface.

The combined effect of the electrolysis of hopping sites and the mobility of the resident counterions causes the concentration gradients between W_1 and W_2 to rapidly become linear (at room temperature the associated relaxation time is estimated to be much less than 1 sec) and the electric field in the PTPB film between W_1 and W_2 to become perfectly screened. The experimentally observed steady-state currents therefore arise exclusively from electronic diffusion driven by the concentration gradient

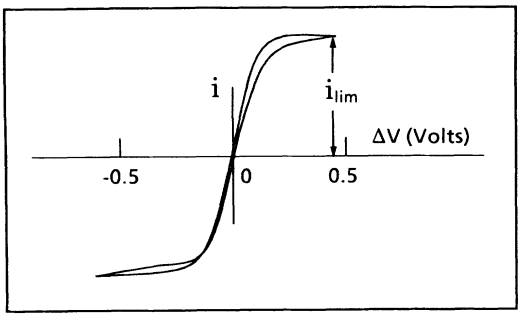

FIG. 9. Solid-state voltammetric curve of the steady-state current i plotted against the interelectrode potential difference (ΔV) in a half-oxidized PTPB film coated onto an IDA which is exposed to acetonitrile vapor.

of radical cations as established by the interelectrode potential difference. In the present case where the PTPB film is 50% preelectrolyzed, the maximum concentration gradient (corresponding to the limiting current) which can be established occurs when the hopping sites are completely oxidized at one electrode interface and completely reduced at the other electrode interface. Thus Eq. (8) is applicable to the calculation of the hole diffusion coefficient from the limiting current in a plot of current versus interelectrode potential difference.

Figure 9 shows the current-voltage data for the diffusion of holes in the solid state in PTPB at 294 K. Equation (8) is used to determine the solid-state hole diffusion coefficient from the limiting-current data. These hole diffusion coefficients will be referred to as solid-state diffusion coefficients $D_{h,ss}$ to distinguish them from the in-electrolyte values D_h. The results are presented as an Arrhenius plot for $D_{h,ss}$ in Fig. 8 curve A. The slope of the plot indicates a solid-state hole hopping activation energy of 0.55 eV. Curve B is the analogous result for D_h. The departure of the solid-state activation energy $D_{h,ss}=0.55$ eV, from the in-electrolyte value $D_h=0.31$ eV, is significant and is discussed below.

D. Comparison of diffusion and mobility

For purposes of comparison we now assume that the electrochemically determined hole diffusion data for PTPB can be expressed as an equivalent zero-field drift mobility via the Einstein relation,

$$\mu_{E=0}=D(e/k_BT)\ , \tag{9}$$

where e is the electronic charge and k_B is the Boltzmann constant. This key comparison with TOF drift mobility data is illustrated in Fig. 10. The solid squares are the TOF drift mobility data extrapolated to zero field as illustrated in Fig. 4. For comparative purposes the zero-field drift mobilities computed via a linear rather than square-root extrapolation, represented by solid triangles, are included. The zero-field hole drift-mobility activation from the square-root extrapolation is 0.53 eV. It is 0.45 eV from the linear extrapolation. The open circles are mobilities computed from the solid-state electrochemical data. Clearly both the absolute values of the mobilities computed from solid-state diffusion data and their temperature dependence agree very well with the experimentally obtained values of hole mobility based on the square-root extrapolation of drift-mobility data.

Although the effective hole mobilities computed from in-electrolyte diffusion data over the temperature range illustrated in Fig. 10 will not differ from the TOF data by more than a factor of 3–5, the effective activation determined from the in-electrolyte data, 0.31 eV, is quite different. The detailed lack of agreement in the comparison involving the effective in-electrolyte mobility, $D_h(e/kT)$, and the experimental zero-field mobilities are thought to be due to important differences in the physical nature of the specimens used in the TOF and in the in-electrolyte studies. The coupling of local or microscopic redox site motions to electron exchange should, in principle, be very important. The nature of the molecular motions in the dry polymer film and in the polymer plasticized with and significantly swelled by acetonitrile electrolyte must be different. It is clear from earlier electrochemical studies[2,3] of films of PTPB that significant swelling of the polymer occurs in the in-electrolyte measurements. It is also well known that polymers contacted with solvating liquids[45,46] and in particular electroactive polymers which are permeated by a contacting liquid electrolyte,[47–49] can be readily plasticized. Thus one might expect a larger degree of motional freedom in both the polymer chain segments and in the electroactive transport sites which are incorporated within the main chain in the in-electrolyte measurements. The latter should result in a lowering of the activation barrier for electron transfer if geometric or steric factors are impor-

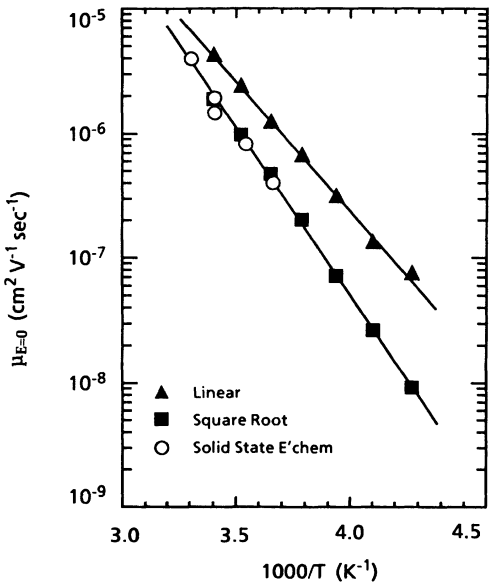

FIG. 10. Arrhenius plots of $\mu_{E=0}$ in PTPB (solid squares, obtained from Fig. 4 zero-field data) compared with mobilities computed from solid-state voltammetric curves (open circles). Solid triangles represent data obtained from a linear field extrapolation.

tant in the elementary electron transfer step. On the other hand, drift-mobility and dry electrochemical diffusion measurements are made on specimens held well below their respective glass transition temperatures. Under these circumstances certain chain segmental and hopping-site motional degrees of freedom present in the imbibed film are clearly frozen out. The experimental hopping activation energies appear to be consistent with this picture.

Because counterion motions are part of any electrochemical measurement, it is necessary to discuss the extent to which these motions are coupled to electronic diffusion in the present case. It should be understood that these counterion motions are not associated with any net transport of mass: in the present electrochemical techniques where steady-state conditions can be maintained indefinitely, there is electronic transport but no net transport of mass (of the counterions). Although an independent determination of the spectrum of counterion motions is not possible, it can nonetheless be established that during the measurement of diffusion coefficients, electronic dissipative processes arising from coupling to such motions, are not significant in PTPB. This was shown earlier[2,3] in comparative measurements of D_h in both uncrosslinked and electrochemically crosslinked PTPB. It is particularly relevant to note that D_h became dramatically higher (a 30-fold increase) in PTPB samples which were crosslinked. Both samples are identical in counterion and transport-site composition, except that in the latter hole transport sites become linked by chemical bonds. Furthermore, it is known that in crosslinked polymer specimens, ionic motion is characteristically inhibited because of film densification. If the rate of microscopic counterion motions (i.e., at a molecular level) is somehow limiting the rate of electron hopping in the uncrosslinked sample, a decrease in the electron hopping rate is expected in the crosslinked samples. In fact, just the opposite was observed. That the electronic hopping rate in fact increases immediately implies that the counterion motions have little bearing on measurements of the hole diffusion coefficients in uncrosslinked samples (those used in this study) as well. Since the respective specimen films used for TOF and solid-state electrochemical diffusion measurements are distinguished only by the presence of counterions in the latter, the validity of the experimental diffusion-mobility comparisons is ensured.

It remains to consider the impact of average intersite separation of a large inclusion of counterions together with the additional swelling induced by permeating acetronitrile vapor. The influence of incorporated counterions on hopping-site concentration has been analyzed theoretically and experimentally by Fritsch-Faules and Faulkner.[50] Their reasoning can be applied to the results of the present study. In PTPB, the average edge-to-edge hopping-site separation along the backbone, 10 Å, cannot be affected by any diluent but some influence on interchain spacing is to be expected. Consider, however, the worst case scenario, namely that of an analogous dispersion of TPD sites in an inert glassy matrix. In the latter case, the concentration of TPD hopping sites would be 1.47×10^{-3} moles/cm^3 (11.5 Å center-center). Upon addition of an equimolar concentration of perchlorate counterions the concentration of TPD sites becomes 1.44×10^{-3} mol/cm^3 (11.62 Å). This minimal effect (an increment of 0.1 Å) is the result of the significantly smaller molar volume of the perchlorate anion ($\sim$15 cm^3/mol) relative to that of the polymer repeat unit (679 cm^3/mol). Under these conditions, applying the model of Fritsch-Faules and Faulkner,[50] an indiscernible change in the hole diffusivity is to be expected. Similarly, assuming a worst case scenario for film swelling by acetonitrile vapor, namely a volume increase of 10%, leads to an increase in the average intersite distance of 11.53 to 11.92 Å, i.e., incremented by 0.4 Å. A volume increase of 5% would lead to an average intersite distance of 11.7 Å, i.e., an increment of 0.2 Å. It is not expected that these minimal changes in intersite distance would lead to experimentally discernible changes in diffusivity.[50]

The agreement of $D_{h,ss}(e/k_BT)$ and $\mu_{E=0}$ clearly demonstrates the validity of the Einstein relation as it applies to a description of the time dependence of the mean position of the advancing carrier packet in the zero-field limit. This is not inconsistent with expectations for a system presumed to be homogeneous, in which a steady-state propagation velocity has been achieved in a small fraction of the experimentally determined transit time. In the usual picture of Gaussian transport involving a sheet of charge at $t=0$, the ratio of thermally driven diffusive spreading Δx to the displacement $\langle x \rangle$ at time t is given by Eq. (10),

$$\langle \Delta x^2 \rangle^{1/2}/\langle x \rangle = (k_BT/eE)(2/Dt)^{1/2} . \quad (10)$$

However, it is found that transit pulse widths computed from the values of $D_{h,ss}$ (experimentally determined from electrochemical measurements) are very much smaller than the typical transit pulse widths which are experimentally observed in TOF measurements on PTPB. For example, under the conditions which apply to Fig. 3, a relative dispersion of $\Delta t/\tau_T=0.002$ is computed from the solid-state hole diffusion data, whereas the relative disperison computed directly from inspection of the

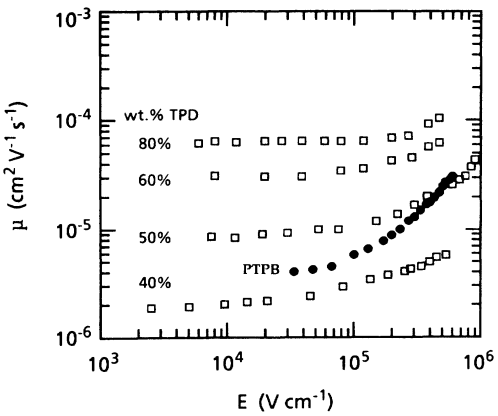

FIG. 11. Logarithm mobility (open squares) plotted against the logarithm of the applied field for various concentrations (wt. %) of TPD in a polycarbonate binder. For comparison the PTPB data are plotted as solid circles.

figure is $\Delta t/\tau_T = 0.3$, a disparity of over two orders of magnitude. While the experimentally observed dispersion of the transit pulses increases with decreasing temperature, as expected, its field dependence is found to be negligible. Fully analogous behavior has already been noted in previous studies on polysilylenes[5] and certain molecularly doped polymers.[8] However, those earlier studies were based solely on diffusion coefficients computed from the Einstein relation and from the drift-mobility data itself. The present study which includes direct measurements of charge-carrier diffusivity both directly verifies conclusions deduced from these earlier observations and supports their generality. Finally, it should be pointed out here that the disorder model, which in fact nominally accounts for the magnitude of the transit pulse width, predicts for PTPB a much greater field dependence than is actually observed.

E. Comparison of hopping in PTPB and an analog molecularly doped polymer

Figure 11 plots the logarithm of the drift mobility against the logarithm of the electric field, comparing the polymer PTPB to various weight percent concentrations of the small molecule *N,N'*-diphenyl-*N,N'*-bis(3-methylphenyl)-[1,1'-biphenyl]-4,4'-diamine (TPD) dispersed in polycarbonate. In both cases at comparable weight percent loadings, bridge measurements of the respective relative low-frequency dielectric constants of these media remain at about 3. This is to be expected from the similarity in the molecular structures of the two systems. The latter dispersions of TPD in polycarbonate made over a wide range of concentrations represent a prototypical system of molecularly doped polymers which have been extensively characterized by the TOF technique.[9] Solid solutions of TPD dispersed in a polycarbonate matrix are found in fact to preserve all of the qualitative characteristics of hole transport in PTPB but, in addition, exhibit the scaling with intersite separation clearly characteristic of hopping among discrete chromophores. What makes this comparison interesting is (1) that both systems share a common transport active moiety and (2) PTPB incorporates the transport-active moiety into the polymer chain while the transport-active moiety in TPD-polycarbonate is freely dissolved in the polymer matrix. The concentration of the transport active sites in PTPB is 72 wt. %. The key point of Fig. 11 is that the drift mobility of holes in PTPB at room temperature is far below the mobility expected for the equivalent molecular dispersion, the latter being bracketed by the 80 wt. % and 60 wt. % curves.

Figure 12 presents the corresponding plot of the hole drift-mobility activation versus the square root of the applied electric field. The figure demonstrates that the hole-transport activation in PTPB is correspondingly higher than it is in the equivalent dispersion. Fully analogous effects have been reported in two other systems in which similar comparisons have been made. The small molecule triphenylamine (TPA), at 30 wt. % loading in polycarbonate, exhibits higher hole drift mobility than the polymer 4-(*N,N'*-diphenylamino)phenyl methylmethacrylate in which the concentration of in-chain TPA groups in 71 wt. %.[51] Similar data is reported[51] in a study comparing *N*-isopropylcarbazole (NIPC), molecularly dispersed in polycarbonate to the pendant polymer PVK.

The pattern of transport behavior suggested by Figs. 11 and 12 may be a manifestation of the molecular-dynamical and conformational constraints which result from the bonding of transport-active moieties into the polymer main chain. It is speculated that physical incorporation into the polymer main chain may significantly increase molecular rotational energy barriers while decreasing the spectrum of molecular-dynamical motions of the transport-active moiety. It in fact appears that the constraints on motional degrees of freedom (relative to those present in the dispersed system) imposed by constraining the hopping sites within the chain backbone drive the activation up and depresses the hole drift mobility. Though the differences observed could in principle be simply associated with systematic differences in the static disorder characteristics of each system, this pattern of behavior could also be taken to clearly suggest the importance of configurational relaxation and reorientation in the hole-transport process.

IV. SUMMARY AND CONCLUSIONS

Dry film electrochemical techniques are combined with TOF drift-mobility measurements to study electronic transport in a model polytetraphenylbenzidine, PTPB, polymer. Hole transport in PTPB proceeds by a thermally activated hopping process among triarylamine moieties. The convoluted field and temperature dependence of the hole drift mobility exhibits features in common with those observed in a broad class of disordered molecular materials. Notable among these is the scaling

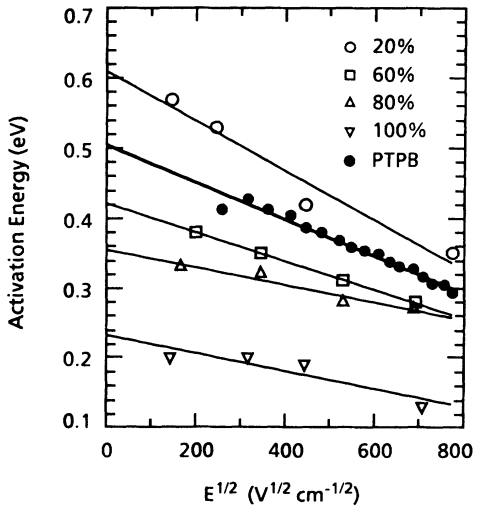

FIG. 12. Hole drift-mobility activation energies (open symbols) plotted against $E^{1/2}$ for various concentrations (wt. %) of TPD in a polycarbonate binder. For comparison the PTPB data are plotted as solid circles.

of the logarithmic mobility with the square root of applied electric field. As a practical matter, this functional behavior has never been verified at fields much below 5×10^3 V/cm in any of these materials. Recent numerical simulation studies predict that a departure from this square-root dependence should onset at low fields. The unique combination of techniques employed here allows the field-dependent behavior of the drift mobility in PTPB to be explored in the zero-field limit. It is found that mobilities computed from solid-state diffusion data using the Einstein relation converge with zero-field TOF drift mobilities obtained by extrapolation from $\log\mu$ vs $E^{1/2}$ plots. Thus the characteristic square-root functional dependence of the logarithm of the drift mobility on electric field is clearly demonstrated to persist through the critical low-field limit. Combining experimentally determined solid-state hole diffusion coefficients with the Einstein relation reveals by an unambiguous and independent route that the dispersion of the transiting charge-carrier packet cannot be accounted for solely on the basis of thermal broadening.

To help elucidate the transport mechanism in PTPB, a careful comparison has been made with a molecular dispersion of TPD in a polycarbonate matrix. The TPD functional group is fully analogous to the transport-active functionality in PTPB. The molecular dispersion and PTPB share the same convoluted pattern of field and temperature dependence. However, it is found that at the same weight percent concentrations of the transport-active moiety, the room-temperature drift mobility is systematically lower and the activation higher when the functional unity is covalently contained within the main chain. The observation of analogous behavior in a variety of disordered systems clearly suggests that a significant role is played by molecular-dynamical and conformational motions in the intersite hopping event.

[1]J. S. Facci and M. Stolka, Philos. Mag. B **54**, 1 (1986).
[2]J. S. Facci, M. A. Abkowitz, W. W. Limburg, D. Renfer, and J. Yanus, Mol. Cryst. Liq. Cryst. **194**, 55 (1991).
[3]J. S. Facci, M. A. Abkowitz, W. W. Limburg, F. Knier, J. Yanus, and D. Renfer, J. Phys. Chem. **95**, 7908 (1991).
[4]J. S. Facci, M. A. Abkowitz, and W. W. Limburg (unpublished).
[5]M. A. Abkowitz, M. J. Rice, and M. Stolka, Philos. Mag. B **61**, 25 (1990).
[6]M. A. Abkowitz, H. Bässler and M. Stolka, Philos. Mag. B **63**, 201 (1991).
[7]M. A. Abkowitz and D. M. Pai, Philos. Mag. B **53**, 193 (1986).
[8]H.-J. Yuh and M. Stolka, Philos. Mag. B **58**, 539 (1988).
[9]M. Stolka, J. F. Yanus, and D. M. Pai, J. Phys. Chem. **88**, 4707 (1984).
[10]H. Bässler, G. Schönherr, M. Abkowitz, and D. M. Pai, Phys. Rev. B **26**, 3105 (1982).
[11]H. Bässler, Philos. Mag. B **50**, 347 (1984).
[12]P. M. Borsenberger, J. Appl. Phys. **68**, 6263 (1990).
[13]P. M. Borsenberger, J. Appl. Phys. **68**, 5682 (1990).
[14]W. D. Gill, J. Appl. Phys. **43**, 5033 (1972).
[15]R. M. Schaffert, *Electrophotography* (Wiley, New York, 1975).
[16]L. B. Schein, A. Peled, and D. Glatz, J. Appl. Phys. **66**, 686 (1989).
[17]L. B. Schein, A. Rosenberg, and S. L. Rice, J. Appl. Phys. **60**, 4287 (1986).
[18]L. B. Schein, Philos. Mag. B **65**, 795 (1992).
[19]L. B. Schein and J. X. Mack, Chem. Phys. Lett. **149**, 109 (1988).
[20]L. B. Schein, Mol. Cryst. Liq. Cryst. **183**, 41 (1990).
[21]J. X. Mack, L. B. Schein, and A. Peled, Phys. Rev. B **39**, 7500 (1989).
[22]M. A. Abkowitz and M. Stolka, Philos. Mag. Lett. **58**, 239 (1988).
[23]M. Abkowitz, *Electronic Transport in Polymers,* in Proceedings of the Fourth International Conference on Hopping and Related Phenomena, Marburg, FRG, 1990 [Philos. Mag. B **65**, 817 (1992) (Special issue)].
[24]L. Pautmeier, R. Richert, and H. Bässler, Synth. Met. **37**, 271 (1990).
[25]A. V. Vannikov, A. U. Kryukov, A. G. Tyurin, and T. S. Zhuravleva, Phys. Status Solidi **115**, K47 (1991).
[26]A. J. Bard and L. R. Faulkner, *Electrochemical Methods: Fundamentals and Applications* (Wiley, New York, 1980), Chap. 5.
[27]J. C. Jernigan and R. W. Murray, J. Am. Chem. Soc. **109**, 1738 (1987).
[28]J. C. Jernigan and R. W. Murray, J. Phys. Chem. **91**, 2030 (1987).
[29]J. C. Jernigan, N. A. Surridge, M. E. Zvanut, M. Silver, and R. W. Murray, J. Phys. Chem. **89**, 4620 (1989).
[30]C. E. D. Chidsey, B. J. Feldman, C. Lundgren, and R. W. Murray, Anal. Chem. **58**, 601 (1986).
[31]B. A. White and R. W. Murray, J. Am. Chem. Soc. **190**, 2576 (1987).
[32]X. Chen, P. He, and L. R. Faulkner, J. Electroanal. Chem. **222**, 223 (1987).
[33]G. P. Kittlesen, H. S. White, and M. S. Wrighton, J. Am. Chem. Soc. **107**, 7373 (1985).
[34]J. W. Thackery, H. S. White, and M. S. Wrighton, J. Phys. Chem. **89**, 5133 (1985).
[35]G. P. Kittlesen, H. S. White, and M. S. Wrighton, J. Am. Chem. Soc. **106**, 7389 (1984).
[36]E. W. Paul, A. J. Ricco, and M. S. Wrighton, J. Phys. Chem. **89**, 1441 (1985).
[37]J. F. Yanus, J. Spiewak, D. Renfer, and W. W. Limburg, U.S. Patent No. 4,806,443 (21, February, 1989).
[38]H. Scher, and E. W. Montroll, Phys. Rev. B **12**, 2455 (1975).
[39]W. D. Gill, J. Appl. Phys. **43**, 5133 (1972).
[40]H. H. Poole, Philos. Mag. **32**, 112 (1926).
[41]M. Stolka, J. F. Yanus, and D. M. Pai, J. Phys. Chem. **88**, 4707 (1984).
[42]T. Holstein, Ann. Phys. (N.Y.) **8**, 325 (1959).
[43]D. Emin, *Electronic and Structural Properties of Amorphous Semiconductors,* edited by P. G. LeComber and J. Mort (Academic, New York, 1973), Chap. 7.
[44]J. C. Jernigan, C. E. D. Chidsey, and R. W. Murray, J. Am. Chem. Soc. **107**, 2824 (1985).
[45]J. M. Gordon, G. B. Rouse, J. H. Gibbs, and W. M. Risen, Jr., J. Chem. Phys. **66**, 4971 (1977).
[46]T. S. Chow, Macromolecules **13**, 362 (1980).
[47]R. W. Murray, in *Electroanalytical Chemistry,* edited by A. J. Bard (Dekker, New York, 1984), Vol. 13, pp. 191–368.
[48]P. J. Peerce and A. J. Bard, J. Electroanal. Chem. **114**, 89

(1980).
[49]K. W. Willman, R. D. Rocklin, R. Nowak, K. Kuo, F. A. Schultz, and R. W. Murray, J. Am. Chem. Soc. **102**, 7629 (1980).
[50]I. Fritsch-Faules, and L. R. Faulkner, J. Electroanal. Chem. **236**, 237 (1989).
[51]M. Stolka, D. M. Pai, D. F. Renfer, and J. F. Yanus, J. Polym. Sci. Polym. Chem. Ed. **21**, 969 (1983).

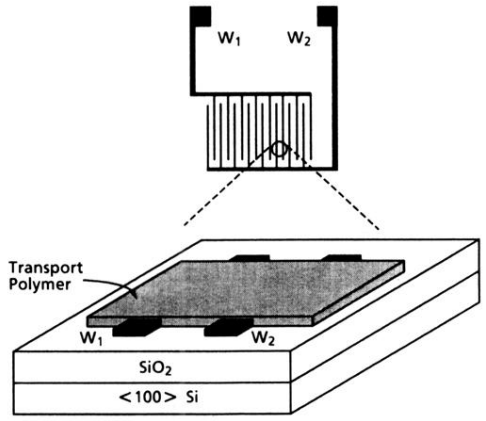

FIG. 2. Schematic diagram of the experimental arrangement for electrochemical measurements of the hole diffusion coefficient in PTPB polymer films. Thin films of PTPB are coated onto a microelectrode interdigitated array.

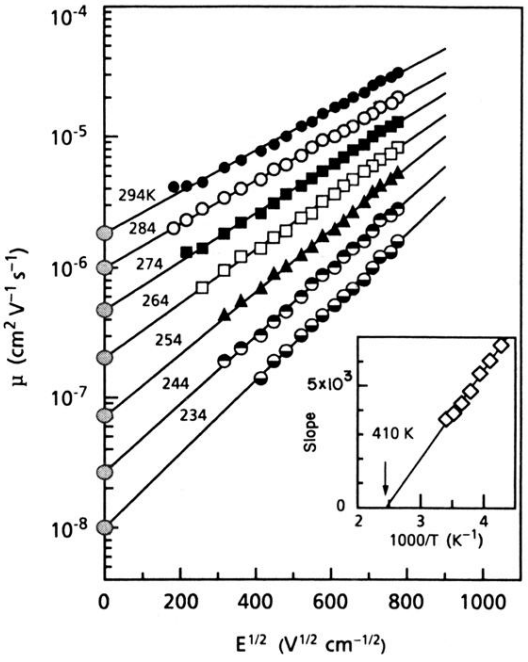

FIG. 4. Logarithm of the TOF drift mobility vs the square root of the applied field at various temperatures. The inset shows the slopes of the logarithmic mobility vs square-root field plots plotted against inverse temperature. A linear fit extrapolates to zero at 410 K.

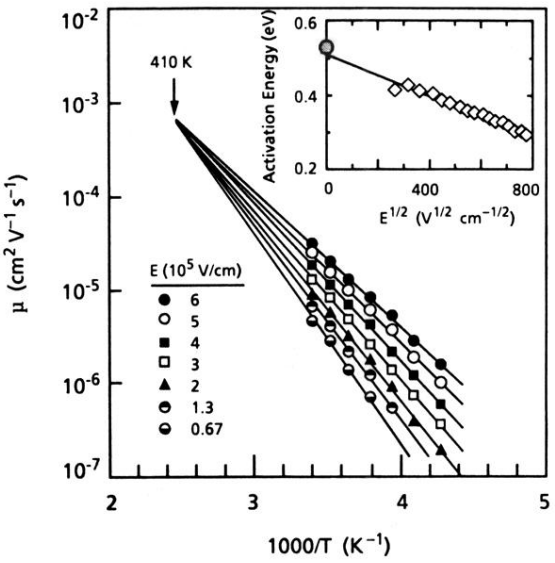

FIG. 5. Arrhenius plots of the TOF hole drift mobility in PTPB. The plots are parametric in the applied field. Inset: activation energies, computed from the slopes of the Arrhenius plots plotted against the square root of the field. The symbol on the zero-field axis is the activation energy determined from an Arrhenius plot of the zero-field data in Fig. 4.